

RESEARCH

Open Access

# Improving the mda-7/IL-24 refolding and purification process using optimized culture conditions based on the structure characteristics of inclusion bodies

Xiaojuan Wang, Chaogang Bai, Jian Zhang, Aiyou Sun\*, Xuedong Wang\* and Dongzhi Wei

## Abstract

**Background:** The melanoma differentiation-associated gene-7 (mda-7)/interleukin-24 (IL-24) can induce apoptosis in a wide variety of tumor cell types, whereas it has no toxicity in normal cells. However, recombinant human mda-7/IL-24 is difficult to obtain from *Escherichia coli* because of its insolubility.

**Results:** In this study, we improved the structure of inclusion bodies (IBs) by optimizing the induction temperature, pH, concentrations of inducer, and metal ion additives. Statistically designed experimental analyses of three metal ion factors were performed using the Box-Behnken design. Induction temperature of 30°C, pH 7.0, and 0.1 mM isopropyl-β-D-thiogalactopyranoside (IPTG) were selected, and the optimized levels for the factors predicted by the model comprised the following: Mg<sup>2+</sup> (15.7 mM), Ca<sup>2+</sup> (16.6 mM), and Mn<sup>2+</sup> (3.0 mM). The optimized culture conditions improved the structure of the IBs, which was validated by scanning electron microscopy (SEM) and the increase of IBs solubility.

**Conclusions:** After optimization, IB solubility and renatured mda-7/IL-24 increased by 51% and 84%, respectively. This study also provided a simple purification method of specific IB washing steps. Manipulating the fermentation parameters to optimize the refolding and purification process is likely to be widely applicable to other proteins.

**Keywords:** *Escherichia coli*; Expression; Inclusion body; Interleukin-24; Purification; Refolding

## Background

The World Cancer Report 2014 emphasized the urgent need for efficient prevention strategies to curb cancer. In 2012, the global cancer burden rose to an estimated 14 million new cases per year, which is expected to rise to 22 million per year within the next 20 years. Thus, studies are searching for the 'Holy grail' of cancer treatment, which can selectively destroy tumor cells without eliciting harmful effects on normal cells or tissues, and melanoma differentiation-associated gene-7 (mda-7)/interleukin-24 (IL-24) appears to be a possible candidate [1]. The mda-7 is a novel tumor cell-specific apoptosis-inducing gene, and it was identified via a subtraction

hybridization approach from human melanoma cells that were stimulated into growth arrest and terminal differentiation by treatment with fibroblasts of IFN and mezerein [2]. Subsequently, mda-7 has been classified as a member of the expanding IL-10 gene family and it was designated as IL-24 [3,4]. mda-7/IL-24 has apoptosis-inducing properties in a broad spectrum of human tumors [5-7]. It also has a potent 'bystander' activity [8], inhibits tumor angiogenesis [9], induces antitumor immunity, and synergizes with radiation and other chemotherapeutic agents [10]. Gene therapy of mda-7/IL-24 is currently undergoing phase II clinical trials [11,12], and it is a promising target in the field of antitumor drug research.

The *Escherichia coli* expression system is most widely used for producing large quantities of recombinant proteins [13]. However, mda-7/IL-24 protein is prone to form pyknotic inclusion bodies (IBs) when expressed in

\* Correspondence: sunaiyou@ecust.edu.cn; xdwang@ecust.edu.cn  
State Key Laboratory of Bioreactor Engineering, East China University of Science and Technology, 130 Meilong Road, Shanghai 200237, People's Republic of China

*E. coli*, which are very difficult to refold [14-16]. Solubilization and renaturation steps have an extremely significant effect on the overall process for preparation of biological active protein. Inefficient solubilization results in the reformation of aggregates during the subsequent renaturation steps [17,18]. Thus, the structural characteristics of IBs could affect their solubilization efficiency [19]. There were many studies about the refolding methods of IBs *in vitro* [20-22]. However, no previous studies have attempted to improve the structure of mda-7/IL-24 IBs by optimizing the culture conditions to facilitate the subsequent IB renaturation and purification process. In this study, we evaluated the correlation between the IB solubilization behavior and culture conditions. Furthermore, we assessed the effects of metal ions of  $Mg^{2+}$ ,  $Ca^{2+}$ , and  $Mn^{2+}$  and their interactions using a statistically designed experiment (Box-Behnken design) and simplified the purification process based on the IB characteristics.

## Materials and methods

### Construction of pET28a-mda-7/IL-24

The entire cDNA of the human mda-7/IL-24 gene [GenBank:NM-006850] was stored in our laboratory. Two oligonucleotide primers were designed, forward (5'-GGGAAT TCCATATGGCCCAGGGCCAAGAATTCCACT-3') and reverse (5'-CCCAAGCTTGGGTCAGAGCTTGTAGAAT TTCTG-3'), to introduce the *Nde* I and *Hind* III restriction endonucleases (Takara Bio Inc., Otsu, Shiga, Japan), respectively. The mda-7/IL-24 gene was obtained by PCR with the primers. The resulting products were subcloned into the pET28a (+) expression vector after double digestion. The recombinant plasmid pET28a-mda-7/IL-24 was transformed into BL21 (DE3) pLysS competent cells. The sequence was confirmed by DNA sequencing (Shanghai Jieli Biotechnology Co., Ltd., Shanghai, China).

### Expression of the recombinant human mda-7/IL-24

The recombinant *E. coli* BL21 (DE3) pLysS was inoculated into 250 mL Luria-Bertani (LB) medium, incubated at 37°C with shaking at 200 rpm. When the  $OD_{600}$  of the cultured medium reached 0.6, the culture was induced with isopropyl- $\beta$ -D-thiogalactopyranoside (IPTG) at a final concentration of 1 mM for 4 h. Further, the cells were harvested by centrifugation at 8,000 $\times g$  for 10 min at 4°C, and the pellets were resuspended in lysis buffer (20 mM Tris, 10 mM EDTA, pH 8.5) before disruption, where the sonication program comprised a series of 200  $\times$  3 s bursts at 300 to 400 W power with a 6-s pause between each burst. The samples were then subjected to centrifugation at 10,000 $\times g$  for 30 min. Protein expression was analyzed by sodium dodecyl sulfate-polyacrylamide gel electrophoresis (SDS-PAGE: 15% separating gel and 4% stacking gel).

### Culture conditions

The effects of the culture conditions were studied, including the induction temperatures (18°C, 25°C, 30°C, and 37°C), pH (6.0, 7.0, 8.0, and 9.0), IPTG concentrations (0.1, 0.5, 1.0, and 1.5 mM), and the addition of different metal ions ( $Mg^{2+}$ ,  $Fe^{3+}$ ,  $Ca^{2+}$ ,  $Na^+$ ,  $NH_4^+$ ,  $Mn^{2+}$ ,  $Cu^{2+}$ , and  $K^+$  at concentrations of 0.50, 1.00, 2.00, and 3.00 g/L). The corresponding compounds were  $MgSO_4$ ,  $Fe_2(SO_4)_3$ ,  $CaCl_2$ ,  $NaCl$ ,  $NH_4Cl$ ,  $MnSO_4 \cdot H_2O$ ,  $CuSO_4 \cdot 5H_2O$ , and  $KCl$ . Each experiment was repeated twice with three replicates.

Furthermore, we optimized the concentrations of the metal ions using a Box-Behnken design [23,24] to minimize the IB solubility. The Design-Expert Software (version 8.0, Stat-Ease Inc., Minneapolis, MN, USA) was used for the experimental design and data analysis. Three variables were designed at three levels, which required 17 experiments. The minimum and maximum levels are described in Table 1. All experiments were performed in triplicate, where the response *Y* represented the average value. The optimal values were obtained by solving the regression equation and analyzing three-dimensional (3D) response surface plots and contour plots.

### Solubility of the IBs

mda-7/IL-24 was produced in different culture conditions using 30 mL LB medium in a 250-mL shaker flask. The IBs were obtained by centrifugation after disruption. The same amount of enriched IBs (1 mg) was resuspended in 1 mL solubilization buffer (8 M urea) and vortexed for 2 h at room temperature. The IB solubility will be affected by their structures, which will result in difference in turbidity when IBs were dissolved in denaturation buffer. The turbidity of IB resuspension in the solubilization buffer was chosen as the index to reflect the solubility of IBs, and lower turbidities were associated with higher IB solubilities [25,26]. The turbidity of the suspension was measured at 480 nm.

The samples were centrifuged at 13,000 $\times g$  for 30 min and filtrated through a 0.45- $\mu m$  Millipore filter (Millipore Co., Billerica, MA, USA). The protein content was estimated by using micro-BCA kit (Beijing Solarbio Science & Technology Co., Ltd., Beijing, China).

**Table 1 Coded values of variables used in Box-Behnken design**

Independent variable name(g/L)	Level		
	-1	0	1
A: $MgSO_4$	1.50	2.00	2.50
B: $CaCl_2$	1.00	1.50	2.00
C: $MnSO_4$	0.50	0.75	1.00

**Table 2 The components of '3 + 1' washing buffers**

Washing buffer	Urea (M)	EDTA (mM)	Tris (mM)	NaCl (mM)	Triton X-100 (%)	pH of the buffer
Buffer I	2	10	20	100	1	8.5
Buffer II	4	10	20	0	2	8.5
Buffer III	2	10	20	0	1	9.5
Deionized water	0	0	0	0	0	6.5 to 7.0

### Washing, denaturation, and refolding of IBs

After disruption, the enriched IBs were solubilized and refolded. mda-7/IL-24 IBs were washed using '3 + 1' washing buffers (about 1 g IBs were solubilized in 30 mL washing buffer): buffer I, buffer II, buffer III, and deionized water (Table 2). In each step, the IBs were resuspended in washing buffer and agitated for 2 h. Then, the IBs were harvested by centrifugation at 10,000×g for 30 min. After these washing steps, high-purity IBs of mda-7/IL-24 were obtained.

Further, the high-purity IBs were dissolved in a buffer solution (20 mM Tris, 10 mM EDTA, and 8 M urea, pH 9.0) and stirred overnight to facilitate denaturation of the mda-7/IL-24 protein. Renatured mda-7/IL-24 protein was achieved by dialysis (the concentration of mda-7/IL-24 was 0.10 mg/mL at the beginning of dialysis) with the decrease of urea concentrations (6, 3, 1.5, 0.75, and 0 M), where each dialysis buffer was applied for 12 h at 4°C with mild agitation. Finally, the bioactive mda-7/IL-24 protein was dialyzed in phosphate-buffered saline (PBS) (50 mM, pH 7.4).

### Western blot assay

The SDS-PAGE analysis was performed using 15% SDS-polyacrylamide gels. The proteins retained in the gels

were detected using Coomassie brilliant Blue R-250 or they were transferred by electrophoresis to nitrocellulose membranes for western blot analysis [27]. The membranes were probed with anti-mda-7/IL-24 polyclonal antibodies (R&D Systems, Minneapolis, MN, USA). A secondary antibody conjugated to horseradish peroxidase was used to enhance the chemiluminescence.

### Scanning electron microscopy

Optimized and non-optimized IBs were also analyzed by scanning electron microscopy (SEM). The IBs after water dialysis were fixed and frozen [19] and dehydrated using a vacuum freeze dryer (Scientz-10N, Ningbo Scientz Biotechnology Co., Ltd., Ningbo City, China). Then, the samples were covered with gold, viewed, and photographed using a scanning electron microscope (S-3400N), Hitachi, Ltd., Chiyoda, Tokyo, Japan).

### MTT assay

Proliferation inhibition was measured based on the 3-(4,5-dimethylazol-2-yl)-2,5-diphenyltetrazolium bromide (MTT) assay. Human breast cancer cell line MCF-7, human malignant melanoma cell line A-375, and normal human lung fibroblast (NHLF) cell line were plated onto 96-well microtiter plates ( $8 \times 10^3$  cells/well) in Dulbecco's modified Eagle's medium (DMEM) supplemented with 10% fetal bovine serum and incubated at 37°C with 5% CO<sub>2</sub>. After 24 h, the cells were treated with mda-7/IL-24 at varying concentrations for 48 h and PBS as control. The surviving cells were detected by adding 20 μL MTT (5 mg/mL) and incubating for 4 h. The resulting absorbance measured at 490 nm was proportional to the number of viable cells.

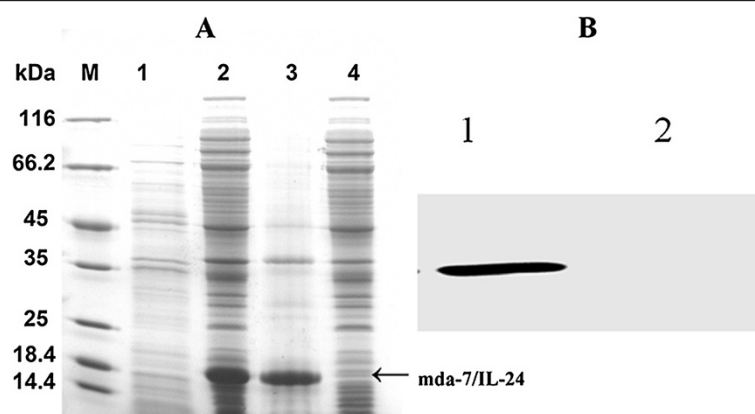


**Figure 1 SDS-PAGE and western blot analysis of mda-7/IL-24. (A)** SDS-PAGE analysis of mda-7/IL-24 expressed in *E. coli*. Lane M, protein molecular weight markers; lanes 1 to 2, whole cell lysate of pET28a-mda-7/IL-24 uninduced and induced; lane 3, insoluble fractions of cell lysate after induction by IPTG; lane 4, soluble fractions of cell lysate after induction by IPTG. **(B)** Western blot analysis of mda-7/IL-24 protein. Lane 1, western blot analysis of mda-7/IL-24; lane 2, blank control without anti-human mda-7/IL-24 antibody.

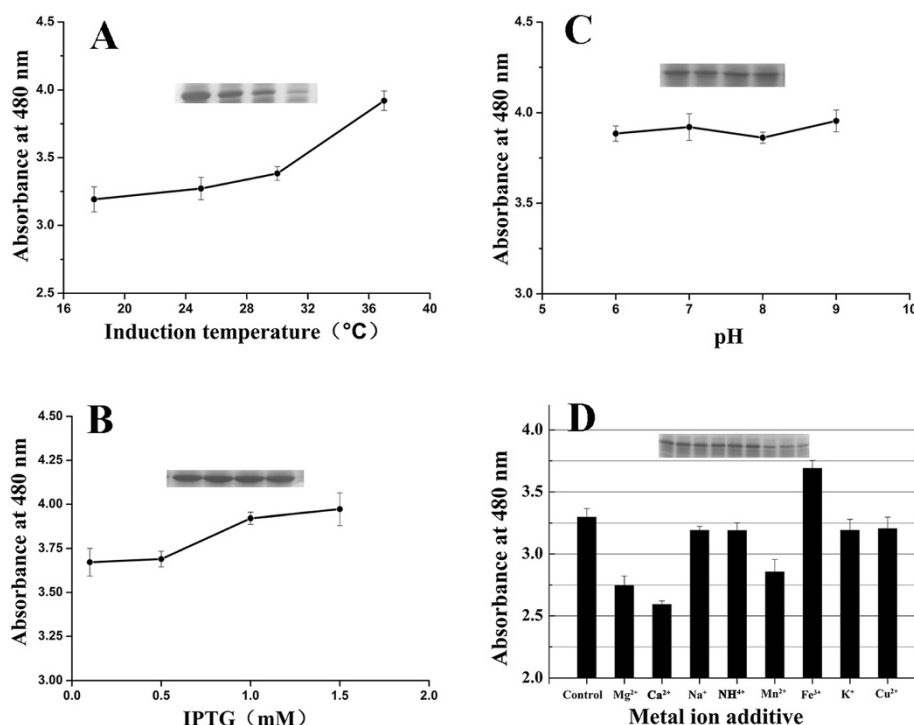


**Figure 2** Influence of culture conditions on mean turbidity ( $\pm$ SD). **(A)** The effects of different induction temperatures on turbidity. **(B)** The effects of different IPTG concentrations on turbidity. **(C)** The effects of different pH values on turbidity. **(D)** The effects of different metal ions (2.00 g/L) on turbidity. The mda-7/IL-24 expressions analyzed by SDS-PAGE in corresponding conditions are placed above each graph.

**Table 3** Box-Behnken design of variables for process optimization

STD order	Factors coded			Response OD <sub>480</sub>	
	A	B	C	Actual value	Predicted value
1	-1	-1	0	3.492	3.562
2	1	-1	0	2.738	2.769
3	-1	1	0	2.274	2.244
4	1	1	0	2.536	2.466
5	-1	0	-1	2.419	2.393
6	1	0	-1	2.203	2.216
7	-1	0	1	2.574	2.561
8	1	0	1	2.139	2.165
9	0	-1	-1	3.319	3.275
10	0	1	-1	1.945	2.002
11	0	-1	1	2.928	2.871
12	0	1	1	2.479	2.523
13	0	0	0	2.013	2.075
14	0	0	0	2.273	2.075
15	0	0	0	1.996	2.075
16	0	0	0	1.892	2.075
17	0	0	0	2.202	2.075

## Results

### Expression of mda-7/IL-24

Recombinant plasmid pET28a-mda-7/IL-24 was obtained successfully, which contained a sequence of 474-bp coding sequence for 158 amino acid residues, and produced approximately 18-kDa protein (Figure 1A). The mda-7/IL-24

**Table 4** Analysis of variance (ANOVA) for quadratic polynomial model

Source	Sum of squares	df	Mean square	F value	Prob > F	Remark
Model	3.3000	9	0.3700	20.8900	0.0003	Significant
A	0.1633	1	0.1633	9.3161	0.0185	Significant
B	1.3146	1	1.3146	74.9956	<0.0001	Significant
C	0.0068	1	0.0068	0.3905	0.5519	
AB	0.2581	1	0.2581	14.7218	0.0064	Significant
AC	0.0120	1	0.0120	0.6840	0.4355	
BC	0.2139	1	0.2139	12.2027	0.0101	Significant
A <sup>2</sup>	0.1295	1	0.1295	7.3897	0.0298	Significant
B <sup>2</sup>	1.0926	1	1.0926	62.3285	<0.0001	Significant
C <sup>2</sup>	0.0291	1	0.0291	1.6607	0.2835	
Residual	0.1227	7	0.0175			
Lack of fit	0.0238	3	0.0079	0.3208	0.8113	Not significant
Pure error	0.0989	4	0.0247			
Cor total	3.4189	16				

protein comprised up to 30% of the total cellular protein, most of which was present as IBs. The western blot analysis confirmed that mda-7/IL-24 was recognized by the anti-IL-24 monoclonal antibody (Figure 1B).

### Culture condition optimization by response surface methodology

The factors that are known to affect the protein solubility include plasmid copy number, culture media, bacterial

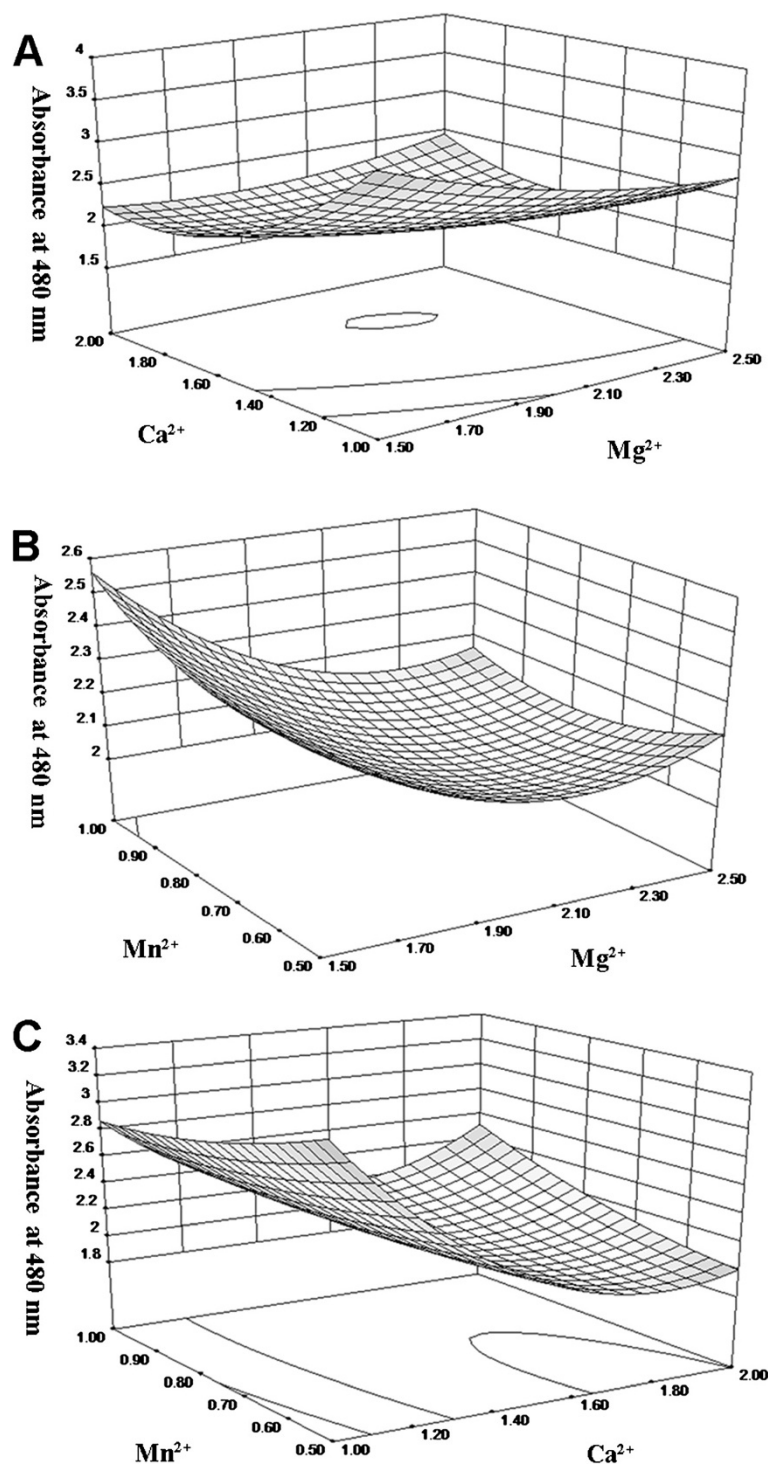


**Figure 3** Three-dimensional response surface curve showing the effects of metal ion additives. (A)  $Mg^{2+}$  and  $Ca^{2+}$ . (B)  $Mg^{2+}$  and  $Mn^{2+}$ . (C)  $Ca^{2+}$  and  $Mn^{2+}$ .



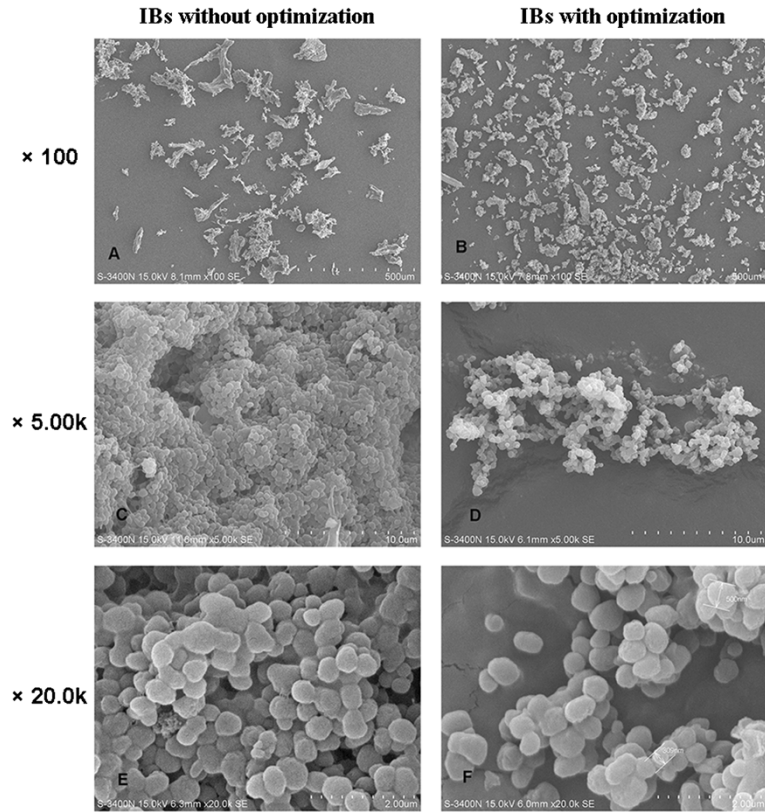


**Figure 4** IB characteristics determined by SEM. (A, C, E) IBs produced before optimization. (B, D, F) IBs produced after optimization.

strain, induction temperature, induction time, and concentration of the inducer [28,29]. We tried to improve the structure of mda-7/IL-24 IBs by optimizing the culture conditions to facilitate the subsequent IB renaturation and purification process. In this study, turbidity was used as a quantitative index of IB solubility. The effects of culture conditions on turbidity are shown in Figure 2. Conditions which could significantly reduce the turbidity of IB suspension without markedly reducing the mda-7/IL-24 protein expression were chosen. As a result, we selected an induction temperature of 30°C, pH 7.0, and 0.1 mM IPTG. Culture additives of Mg<sup>2+</sup>, Ca<sup>2+</sup>, and Mn<sup>2+</sup> had positive effects on reducing the turbidity compared with the control, where the turbidity was decreased by 11%, 16%, and 7.0%, respectively. In contrast, Na<sup>+</sup>, NH<sub>4</sub><sup>+</sup>, K<sup>+</sup>, and Cu<sup>2+</sup> had no obvious effects, whereas Fe<sup>3+</sup> increased the turbidity greatly.

To achieve the maximum solubilization of mda-7/IL-24 IBs, we optimized the IB turbidity using the Box-Behnken design, which included metal ion additives, i.e., (A) Mg<sup>2+</sup>, (B) Ca<sup>2+</sup>, and (C) Mn<sup>2+</sup>. The design matrix and the results of the 17 experiments conducted using the Box-Behnken design are described in Table 3, which comprised 12 trials plus five center points. The results obtained were analyzed by ANOVA using the Design-

Expert Software (version 8.0 Stat-Ease Inc.). The regression model used was as follows:

$$Y(OD_{480}) = +16.38667 - 4.28765A - 10.34305B - 3.77760C + 1.01600AB - 0.43800AC + 1.85000BC + 0.70160A^2 + 2.03760B^2 + 1.33040C^2 \quad (1)$$

**Table 5** The simplified purification process of the washing steps

Washing step	Total protein (mg)	mda-7/IL-24 (mg)	mda-7/IL-24 yield (%)	mda-7/IL-24 purity (%)
Before washing	105	68	-	65
Buffer I	84	61	89	73
Buffer II	65	56	92	86
Buffer III	53	49	88	92
Deionized water	50	48	98	96

The wet weight of the *E. coli* cells was 3.75 g from 1 L culture medium, and 105 mg IBs was obtained after disruption. mda-7/IL-24 comprised up to 30% of the total protein. The total target protein lost 29% during the washes and 8.4% during the dialysis. The final purity of mda-7/IL-24 was about 95%.

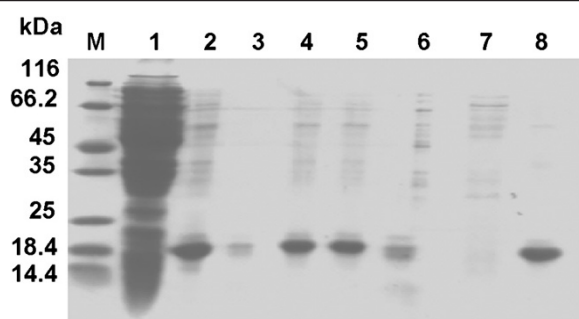


**Figure 5** The SDS-PAGE analysis of mda-7/IL-24 after '3 + 1' washing steps. Lane M, protein molecular weight markers; lane 1, supernatant of bacteria lysate; lanes 2, 4, and 5, pellets washed by washing buffers I, II, III, respectively; lanes 3, 6, 7, supernatants after each wash steps (I, II, and III wash steps, respectively); lane 8, the final pellets after '3 + 1' washing steps.

The results of the ANOVA for the regression model are shown in Table 4. The model  $F$  value of 20.89 implied that the model was significant, i.e., there was only a 0.03% chance that a 'model  $F$  value' this large could occur due to noise. The coefficient of determination ( $R^2$ ) was used to check the goodness of fit of the model (Table 4), where  $R^2$  was 0.9641. The value of the adjusted coefficient of determination (adjusted  $R^2 = 0.9180$ ) agreed reasonably well with the predicted  $R^2$  (0.8434). The lack-of-fit value for the regression of Equation 1 was not significant (0.8113), thereby indicating that the model equation was suitable for predicting the turbidity with any combination of values for the variables. 'Adeq Precision' measures the signal-to-noise ratio, where a ratio greater than four is considered to be desirable [30]. The 'Adeq Precision' ratio of 15.336 obtained in the present study indicated an adequate signal. Thus, this model can be used to navigate the design space.

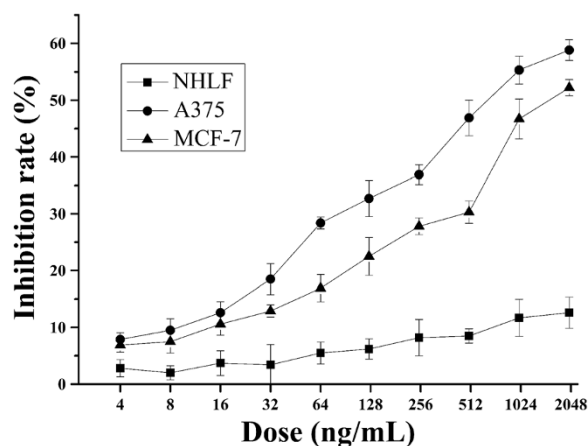


**Figure 6** The activity of renatured mda-7/IL-24 ( $\pm$ SD). mda-7/IL-24 inhibits the survival of A375 and MCF-7 cells in a concentration-dependent manner, whereas it has little effect on the growth of NHLFs.

**Table 6** Solubilization and refolding before and after optimization

Optimization items	Solubilization		Refolding	
	Absorbance at 480 nm	Increase of solubility (%)	Renatured mda-7/IL-24 (%)	Increase of refolding (%)
Control	3.921	-	13	-
Temperature	3.383	14	16	22
IPTG	3.672	6	14	9.0
pH	Not significant	-	-	-
Metal ion additives	1.94	51	23	84

The effects of the addition of metal ions, i.e., (A)  $Mg^{2+}$ , (B)  $Ca^{2+}$ , and (C)  $Mn^{2+}$ , on IB solubilization were visualized using 3D response surface and contour plots in (Figure 3). The 3D graphs were generated based on the response of pairwise combinations of the three factors while keeping the other at its optimum level. The graphs are shown to demonstrate the effects of various factors on the turbidity. The interaction effect of  $Mg^{2+}$  and  $Ca^{2+}$  is shown in Figure 3A.  $Ca^{2+}$  exhibited a quadratic response and it was the major factor, while  $Mg^{2+}$  also exhibited a quadratic response. These data suggested that the  $Mg^{2+}$  and  $Ca^{2+}$  had significant effects on turbidity, and they also had significant interaction effects on each other. The interaction effect of  $Mg^{2+}$  and  $Mn^{2+}$  is shown in Figure 3B. The effects of  $Mn^{2+}$  and its quadratic response were not significant, while  $Mg^{2+}$  and  $Mn^{2+}$  also had non-significant interaction effects on each other. However,  $Ca^{2+}$  and  $Mn^{2+}$  had significant interaction effects on each other, where the

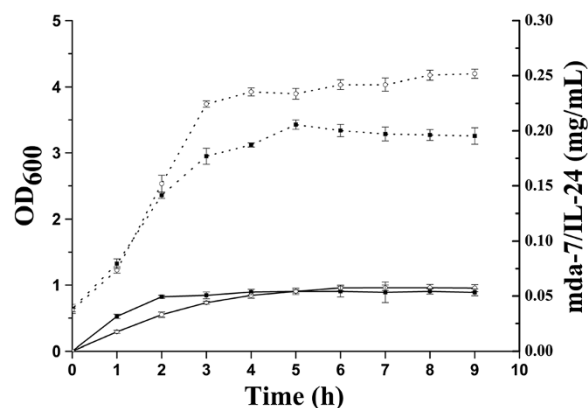


**Figure 7** Bacteria growth ( $OD_{600}$ ) and mda-7/IL-24 protein production (mg/mL) before and after optimization. *E. coli* were grown in a 30 mL culture medium. Dotted lines represent values of mean  $OD_{600}$  ( $\pm$ SD), without optimization (...■...) and with optimization (...○...). Solid lines represent values of protein production ( $\pm$ SD), without optimization (—■—) and after optimization (—○—).

effect of  $\text{Ca}^{2+}$  was enhanced in the presence of  $\text{Mn}^{2+}$  (Figure 3C).

A validation was performed using the conditions predicted by the model. The optimized levels predicted by the model were as follows:  $\text{Mg}^{2+}$  (15.7 mM),  $\text{Ca}^{2+}$  (16.6 mM), and  $\text{Mn}^{2+}$  (3.0 mM). The predicted turbidity was 1.92 (suspension measured at 480 nm), and the actual obtained was 1.94. The exact correlation between the experimental and predicted values validated this model.

#### IB characteristics determined by SEM

The structures of the IBs were also examined by SEM (Figure 4). It was clear that IBs without optimization were much larger, and the particles stuck together tightly (Figure 4A,C,E). While IBs with optimization had a more regular shape and appeared to be much looser, even single particles could be observed (Figure 4B,D,F).

#### Simplified purification process

In our study, IBs comprised up to approximately 100% of the total mda-7/IL-24 even after these optimizations. mda-7/IL-24 IBs were barely dissolved in both 8 M urea and 6 M guanidine hydrochloride. A '3 + 1' IB washing process was designed. High concentration of urea and Triton X-100 could effectively remove the impurities, while the pyknotic mda-7/IL-24 IBs were not completely removed in the washing steps. The purity of mda-7/IL-24 after '3 + 1' steps was 96% (Table 5, Figure 5). This was a simplified purification process, which required no additional procedures, such as affinity chromatography purification.

#### Bioactivity of mda-7/IL-24

The results showed that mda-7/IL-24 had negligible inhibitory effects on NHLF cells, while it had cytotoxicity effects on MCF-7 cells and A375 cells in a concentration-dependent manner, and the 50% inhibitory concentrations were about 1.0 and 0.7  $\mu\text{g/mL}$ , respectively (Figure 6).

#### Conclusions

Recombinant protein is prone to form IBs when expressed in *E. coli*. Recombinant human mda-7/IL-24 IBs are difficult to refold due to its low solubility [14]. Some studies tried to obtain soluble expression or easy refolding of mda-7/IL-24 using genetic methods [15,16,31]. However, no previous study has attempted to improve the structure of mda-7/IL-24 IBs by optimizing the culture conditions to facilitate the subsequent IB renaturation and purification. In this study, culture conditions were optimized, which increased the solubility of mda-7/IL-24 IBs by approximately 51% (Table 6). We speculated that the optimized culture conditions improved the IB structure, which was validated by SEM and the increase of solubility.

The renatured protein almost had the same activity as the commercial product of mda-7/IL-24 (Cloud-Clone Corp., Houston, TX, USA) expressed in *E. coli*. Therefore, we confirmed the activities of the renatured mda-7/IL-24 protein and did not evaluate the proportion of the active proteins. Efficient solubilization could contribute to the performance of the subsequent renaturation steps [17,18], and the renatured mda-7/IL-24 protein increased by 84% in our experiments (Table 6).

The '3 + 1' washing steps could gradually remove the miscellaneous proteins and also make the IB particles loose, which benefited the subsequent refolding process. As a result, the purity of mda-7/IL-24 was 96% after '3 + 1' washing steps. Therefore, the '3 + 1' washing approach based on these IB structural characters was a simplified purification process.

With the optimized conditions, the mda-7/IL-24 formation rate was slower during the early stage and faster during the late stage (Figure 7). This may be due to some proteins being synthesized in the early stage that facilitated the correct folding of the mda-7/IL-24 protein, thereby allowing the IBs to possess a greater proportion of native-like secondary structure [32]. Therefore, the structure of IBs was improved and the solubility of the IBs increased. It is an important method to optimize the renaturation and purification process by manipulating the fermentation parameters [33]. This approach may also be applied to the expression of other proteins with similar structural characteristics.

#### Competing interests

The authors declare that they have no competing interests.

#### Authors' contributions

XJW and CB carried out the molecular genetic studies, participated in the sequence alignment, and drafted the manuscript. XJW and JZ participated in the design of the study and performed the statistical analysis. AS, XDW, and DW conceived of the study, participated in its design and coordination, and helped draft the manuscript. All authors read and approved the final manuscript.

#### Acknowledgements

This work was supported by a grant from the Ministry of Science and Technology (National Major Science and Technology Projects of China (No. 2012ZX09304009)).

Received: 20 August 2014 Accepted: 16 October 2014

Published online: 12 November 2014

#### References

1. Fisher PB (2005) Is mda-7/IL-24 a "magic bullet" for cancer? *Cancer Res* 65:10128–10138
2. Jiang H, Lin JJ, Su ZZ, Goldstein NI, Fisher PB (1995) Subtraction hybridization identifies a novel melanoma differentiation associated gene, mda-7, modulated during human melanoma differentiation, growth and progression. *Oncogene* 11:2477–2486
3. Caudell EG, Mumm JB, Poindexter N, Ekmekcioglu S, Mhashilkar AM, Yang XH, Retter MW, Hill P, Chada S, Grimm EA (2002) The protein product of the tumor suppressor gene, melanoma differentiation-associated gene 7, exhibits immunostimulatory activity and is designated IL-24. *J Immunol* 168:6041–6046
4. Chada S, Sutton RB, Ekmekcioglu S, Ellerhorst J, Mumm JB, Leitner WW, Yang HY, Sahin AA, Hunt KK, Fuson KL, Poindexter N, Roth JA, Ramesh R,



- Grimm EA, Mhashilkar AM (2004) mda-7/IL-24 is a unique cytokine-tumor suppressor in the IL-10 family. *Int Immunopharmacol* 4:649–667
5. Su Z-Z, Madireddi MT, Lin JJ, Young CS, Kitada S, Reed JC, Goldstein NI, Fisher PB (1998) The cancer growth suppressor gene mda-7 selectively induces apoptosis in human breast cancer cells and inhibits tumor growth in nude mice. *Proc Natl Acad Sci* 95:14400–14405
6. Ekmekcioglu S, Ellerhorst J, Mhashilkar AM, Sahin AA, Read CM, Prieto VG, Chada S, Grimm EA (2001) Down-regulated melanoma differentiation associated gene (mda-7) expression in human melanomas. *Int J Cancer* 94:54–59
7. Lebedeva IV, Sarkar D, Su Z-Z, Kitada S, Dent P, Stein C, Reed JC, Fisher PB (2003) Bcl-2 and Bcl-x(L) differentially protect human prostate cancer cells from induction of apoptosis by melanoma differentiation associated gene-7, mda-7/IL-24. *Oncogene* 22:8758–8773
8. Su Z, Emdad L, Sauane M, Lebedeva IV, Sarkar D, Gupta P, James CD, Randolph A, Valerie K, Walter MR (2005) Unique aspects of mda-7/IL-24 antitumor bystander activity: establishing a role for secretion of mda-7/IL-24 protein by normal cells. *Oncogene* 24:7552–7566
9. Ramesh R, Mhashilkar AM, Tanaka F, Saito Y, Branch CD, Sieger K, Mumm JB, Stewart AL, Boquio A, Dumoutier L (2003) Melanoma differentiation-associated gene 7/interleukin (IL)-24 is a novel ligand that regulates angiogenesis via the IL-22 receptor. *Cancer Res* 63:5105–5113
10. Dent P, Yacoub A, Grant S, Curie DT, Fisher PB (2005) mda-7/IL-24 regulates proliferation, invasion and tumor cell radiosensitivity: a new cancer therapy? *J Cell Biochem* 95:712–719
11. Tong AW, Nemunaitis J, Su D, Zhang Y, Cunningham C, Senzer N, Netto G, Rich D, Mhashilkar A, Parker K (2005) Intratumoral injection of INGN 241, a nonreplicating adenovector expressing the melanoma-differentiation associated gene-7 (mda-7/IL24): biologic outcome in advanced cancer patients. *Mol Ther* 11:160–172
12. Azab B, Dash R, Das SK, Bhutia SK, Shen XN, Quinn BA, Sarkar S, Wang XY, Hedvat M, Dmitriev IP (2012) Enhanced delivery of mda-7/IL-24 using a serotype chimeric adenovirus (Ad. 5/3) in combination with the Apogossypol derivative BI-97C1 (Sabutoclax) improves therapeutic efficacy in low CAR colorectal cancer cells. *J cell Physiol* 227:2145–2153
13. Chen R (2012) Bacterial expression systems for recombinant protein production: *E. coli* and beyond. *Biotechnol Adv* 30:1102–1107
14. Ma Q, Jiang H, Liu K, Zhu J, Zheng X (2004) Cloning of human interleukin 24 (mda-7/IL-24) gene and its fusion protein expression in *E. coli*. *Jun Shi Yi Xue Ke Xue Yuan Yuan Kan* 28:221–224
15. Yang J, Zhang W, Liu K, Jing S, Guo G, Luo P, Zou Q (2007) Expression, purification, and characterization of recombinant human interleukin 24 in *Escherichia coli*. *Protein Expression Purif* 53:339–345
16. Liu J-J, Zhang B-F, Yin X-X, Pei D-S, Yang Z-X, Di J-H, Chen F-F, Li H-Z, Xu W, Wu Y-P (2012) Expression, purification, and characterization of RGD-mda-7, a HIS-TAGGED mda-7/IL-24 mutant protein. *J Immunoassay Immunochem* 33:352–368
17. Singh SM, Panda AK (2005) Solubilization and refolding of bacterial inclusion body proteins. *J Biosci Bioeng* 99:303–310
18. Petrides D, Cooney CL, Evans LB, Field RP, Snoswell M (1989) Bioprocess simulation: an integrated approach to process development. *Comput Chem Eng* 13:553–561
19. Kang H, Sun AY, Shen YL, Wei DZ (2007) Refolding and structural characteristic of TRAIL/Apo2L inclusion bodies from different specific growth rates of recombinant *Escherichia coli*. *Biotechnol Prog* 23:286–292
20. Chura-Chambi RM, Cordeiro Y, Malavasi NV, Lemke LS, Rodrigues D, Morganti L (2013) An analysis of the factors that affect the dissociation of inclusion bodies and the refolding of endostatin under high pressure. *Process Biochem* 48:250–259
21. Hayashi M, Iwamoto S, Sato S, Sudo S, Takagi M, Sakai H, Hayakawa T (2013) Efficient production of recombinant cystatin C using a peptide-tag, 4AaCter, that facilitates formation of insoluble protein inclusion bodies in *Escherichia coli*. *Protein Expression Purif* 88:230–234
22. Senthil K, Gautam P (2010) Expression and single-step purification of mercury transporter (merT) from *Cupriavidus metallidurans* in *E. coli*. *Biotechnol Lett* 32:1663–1666
23. Ferreira SC, Bruns R, Ferreira H, Matos G, David J, Brandao G, da Silva EP, Portugal L, Dos Reis P, Souza A (2007) Box-Behnken design: an alternative for the optimization of analytical methods. *Anal Chim Acta* 597:179–186
24. Mao X, Shen Y, Yang L, Chen S, Yang Y, Yang J, Zhu H, Deng Z, Wei D (2007) Optimizing the medium compositions for accumulation of the novel FR-008/Candidin derivatives CS101 by a mutant of *Streptomyces sp.* using statistical experimental methods. *Process Biochem* 42:878–883
25. Singh SM, Upadhyay AK, Panda AK (2008) Solubilization at high pH results in improved recovery of proteins from inclusion bodies of *E. coli*. *J Chem Technol Biotechnol* 83:1126–1134
26. Patra AK, Mukhopadhyay R, Mukhija R, Krishnan A, Garg LC, Panda AK (2000) Optimization of inclusion body solubilization and renaturation of recombinant human growth hormone from *Escherichia coli*. *Protein Expression Purif* 18:182–192
27. Welinder C, Ekblad L (2011) Coomassie staining as loading control in Western blot analysis. *J Proteome Res* 10:1416–1419
28. Correa A, Oppizzo P (2011) Tuning different expression parameters to achieve soluble recombinant proteins in *E. coli*: advantages of high-throughput screening. *Biotechnol J* 6:715–730
29. Vincentelli R, Cimino A, Geerlof A, Kubo A, Satou Y, Cambillau C (2011) High-throughput protein expression screening and purification in *Escherichia coli*. *Methods* 55:65–72
30. Anderson MJ, Whitcomb PJ (2005) RSM simplified: optimizing processes using response surface methods for design of experiments. Productivity Press, Oxon
31. Xiao B, Li W, Yang J, Guo G, Mao XH, Zou QM (2009) RGD-IL-24, a novel tumor-targeted fusion cytokine: expression, purification and functional evaluation. *Mol Biotechnol* 41:138–144
32. Shivu B, Seshadri S, Li J, Oberg KA, Uversky VN, Fink AL (2013) Distinct  $\beta$ -sheet structure in protein aggregates determined by ATR-FTIR spectroscopy. *Biochemistry* 52:5176–5183
33. Shen YL, Xia XX, Zhang Y, Liu JW, Wei DZ, Yang SL (2003) Refolding and purification of Apo2L/TRAIL produced as inclusion bodies in high-cell-density cultures of recombinant *Escherichia coli*. *Biotechnol Lett* 25:2097–2101

doi:10.1186/s40643-014-0021-9

**Cite this article as:** Wang et al.: Improving the mda-7/IL-24 refolding and purification process using optimized culture conditions based on the structure characteristics of inclusion bodies. *Bioresources and Bioprocessing* 2014 **1**:21.

**Submit your manuscript to a SpringerOpen<sup>®</sup> journal and benefit from:**

- Convenient online submission
- Rigorous peer review
- Immediate publication on acceptance
- Open access: articles freely available online
- High visibility within the field
- Retaining the copyright to your article

Submit your next manuscript at ► [springeropen.com](http://springeropen.com)